

Atomically Abrupt Liquid-Oxide Interface Stabilized by Self-Regulated Interfacial Defects: The Case of Al/Al₂O₃ Interfaces

Joongoo Kang,^{1,*} Junyi Zhu,¹ Calvin Curtis,¹ Daniel Blake,¹ Greg Glatzmaier,¹ Yong-Hyun Kim,² and Su-Huai Wei¹

¹National Renewable Energy Laboratory, Golden, Colorado 80401, USA

²Graduate School of Nanoscience and Technology (WCU), KAIST, Daejeon 305-701, Korea

(Received 17 November 2011; revised manuscript received 18 January 2012; published 30 May 2012)

The atomic and electronic structures of the liquid Al/(0001) α -Al₂O₃ interfaces are investigated by first-principles molecular dynamics simulations. Surprisingly, the formed liquid-solid interface is always atomically abrupt and is characterized by a transitional Al layer that contains a fixed concentration of Al vacancies (~ 10 at.%). We find that the self-regulation of the defect density in the metal layer is due to the fact that the formation energy of the Al vacancies is readjusted in a way that opposes changes in the defect density. The negative-feedback effect stabilizes the defected transitional layer and maintains the atomic abruptness at the interface. The proposed mechanism is generally applicable to other liquid-metal/metal-oxide systems, and thus of significant importance in understanding the interface structures at high temperature.

DOI: 10.1103/PhysRevLett.108.226105

PACS numbers: 68.08.-p, 71.15.Nc, 73.20.-r

Structural and electronic properties of metal/oxide interfaces are of great fundamental and technological interest in materials science. Recently, the interfaces between liquid metals and solid oxides have attracted increasing attention due to their roles in high-temperature applications [1–6]. For example, liquid metals protected by thermally stable oxide materials—such as metal/oxide core-shell nanoparticles—have great potential to be used as novel phase-change materials (PCMs) for thermal energy storage and phase-change memory [1,2]. For these nanoscale PCMs, the nanosize effects on their thermal properties such as melting point and latent heat are largely determined by the nature of the metal/oxide interfaces [3–6]. Also, it is now well established from experiments and atomistic simulations that a few ordered liquid layers are formed near the liquid metal/oxide interface [7–10]. Hence, the practical use of the nano-PCMs at high temperature requires microscopic understanding of the liquid-metal/oxide interfaces and the liquid layering effect.

The liquid-metal/oxide interfaces also act as a growth front for the vapor-liquid-solid growth of oxide nanowires. Recently, using *in situ* high-resolution transmission electron microscopy (HRTEM) Oh and his colleagues [9,11] elegantly showed that when Al liquid droplets are formed on a (0001) α -Al₂O₃ single crystal, self-catalytic vapor-liquid-solid growth of α -Al₂O₃ nanowires occurs in a layer-by-layer fashion. The HRTEM images [11] suggest atomically abrupt liquid-solid interfaces, in which a few liquid Al interface layers are in direct contact with the Al-terminated Al₂O₃. However, the in-plane structure of the interfaces is not resolved. For better understanding and control of the epitaxial growth of the Al₂O₃ nanowires, it is also crucial to understand the structural and electronic properties of the liquid Al/Al₂O₃ interfaces.

In this Letter, we report on our first-principles density functional calculations of liquid Al/(0001) α -Al₂O₃ interfaces. We found that the liquid-solid interface is always atomically abrupt, and includes a honeycomblike transitional Al layer between the two different domains. Surprisingly, the transitional Al layer contains a large number of Al vacancies with nearly fixed concentration (~ 10 at.%) and it remains stable even at high temperature. Because of this strong self-regulating tendency, the abruptness of the liquid-solid interface is preserved. Based on our understanding of this unique interfacial structure, we propose an atomistic oxidation process of the liquid Al at the interface in a layer-by-layer fashion during growth.

Computational method.—We performed first-principles molecular dynamics (MD) simulations of a liquid Al nanofilm with a thickness of $t_{\text{Al}} = 2.64$ nm, which is sandwiched between two α -Al₂O₃ (0001) bulk layers [Fig. 1(a)]. To simulate the liquid-solid interfaces, we employed supercells with a periodicity of $1.43 \text{ nm} \times 1.66 \text{ nm}$ for the directions parallel to the interface. The lateral periodicity is commensurate with the bulk α -Al₂O₃ (0001) lattice planes. We confirmed that MD simulations with a doubled supercell in the lateral direction led to essentially the same interfacial structures as in the case of the smaller supercell. The density of Al atoms in the nanofilm was selected to be the same as that of bulk liquid Al at its melting point ($\rho = 2.4 \text{ g/cm}^3$). Total energies were calculated within the generalized gradient approximation [12] to the density functional theory (DFT) for better description of rapid change of electron density near the interfaces, as implemented in the VASP package [13]. Our DFT calculations employed the projector augmented wave method [14,15]. For MD simulations at constant temperatures, the Nosé thermostat [16] was used, and the time step was chosen to be 3 fs. Our test

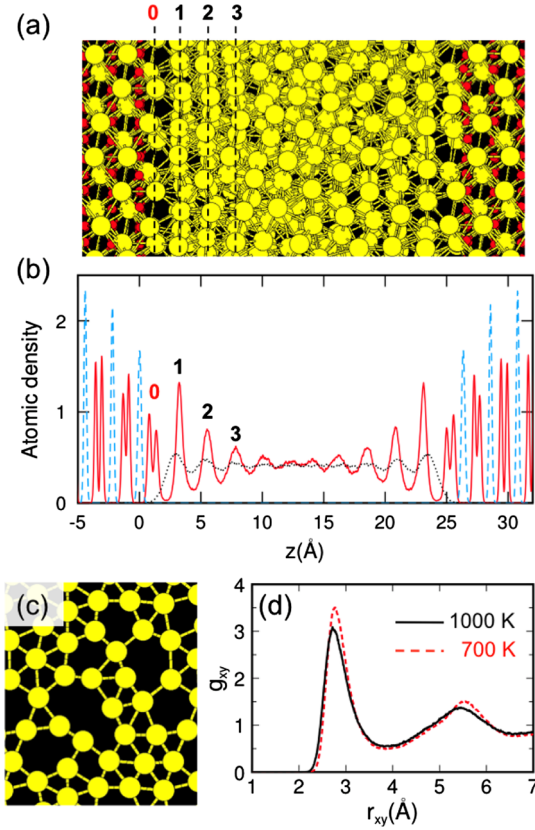


FIG. 1 (color online). Two-dimensional liquid Al layers at the interface with α - Al_2O_3 . (a) A snapshot of the liquid Al layers near the liquid-solid interfaces taken from a first-principles MD simulation at $T = 1000$ K. Large and small balls represent Al and O atoms, respectively. (b) Atomic density plots, which are averaged in planes parallel to the interfaces, are shown for Al atoms (solid red line) and O atoms (dashed blue line) along the z direction perpendicular to the interfaces. The position of the first oxygen layer at the left interface is set to zero. For comparison, a plane-averaged density plot of the Al atoms in a freestanding Al film is also presented (dotted black line). (c) A representative snapshot of the first liquid layer (denoted by 1) at $T = 1000$ K, elucidating a disordered in-plane atomic structure. (d) Simulated lateral Al-Al radial distribution functions g_{xy} of the first liquid layer versus the lateral position r_{xy} .

calculations have shown that this time step is sufficient for accurate calculations of thermal properties of Al films and nanoclusters [17,18] at high temperature. As an initial structure, we constructed an interface structure between the O-terminated (0001) Al_2O_3 and the isotropic, homogeneous liquid Al taken from a separate MD simulation of bulk Al. Then, the interface structure was optimized by using MD simulations at $T = 1000$ K over 100 ps. At $T = 1000$ K, the strong self-regulation mechanism at the interfacial region enables the system to rapidly reach equilibrium, and thus the simulation time is sufficient. Structural analyses were done at $T = 700, 800, 900$, and 1000 K with a sampling time of about 80 ps at each temperature [19].

Ordered liquid Al layers at the interface with α - Al_2O_3 .—Figure 1(a) shows a snapshot of the Al/ Al_2O_3 interfaces at $T = 1000$ K. From the MD structures, we simulated the atomic density profiles for Al (solid line) and O (dashed line) atoms, which are averaged in planes parallel to the interface [Fig. 1(b)]. The oscillatory density profile in the liquid Al region (denoted by 1, 2, and 3) clearly shows that a few liquid layers are formed near the interface. The layering effect decays rapidly with depth from the interface. The simulated density profiles agree reasonably well with the average-intensity line of the HRTEM images obtained in Ref. [9]. Despite the vertical layered structure near the interface, no apparent in-plane order was found in these liquidlike layers, as demonstrated by the representative snapshot in Fig. 1(c) and the simulated lateral Al-Al radial distribution functions g_{xy} of the first liquid layer in Fig. 1(d). For comparison, we also calculated the atomic density profile of a freestanding Al nanofilm. The reduced amplitude in the oscillatory density profile near the surface indicates that the liquid layering effect at the free surface is much weakened.

High concentration of intrinsic Al vacancies at the Al/ Al_2O_3 interface.—The index 0 in the simulated atomic structure and the atomic density plot corresponds to a transitional Al layer, which is adjacent to the first liquid layer (denoted by 1 in Fig. 1). The Al-terminated Al_2O_3 at the liquid-solid interface is consistent with the proposed atomic model from the comparison of the experimental and simulated HRTEM images [11]. Previous DFT calculations [20] also predicted the Al termination for Al(111)/ α - Al_2O_3 (0001) solid-solid interfaces. The Al atoms in the transitional layer participate *both* in the bonding with the oxygen atoms in the O-terminated (0001) Al_2O_3 plane and in forming the metallic liquid with the Al atoms in the liquid layer. As in the Al layers in the bulk α - Al_2O_3 , the in-plane atomic order of the transitional Al layer is a honeycombl-like lattice consisting of two sublattices that are slightly displaced from each other (Fig. 1). Interestingly, the transitional Al layer contains a high concentration of Al vacancies of about 10 at. %, as shown in Fig. 2(a). Because the Al atoms in the inner sublattice more tightly bond to the oxygen atoms in Al_2O_3 , the Al vacancies are distributed exclusively on the outer sublattice that is adjacent to the first liquid layer. More importantly, the density of the Al vacancies is highly regulated with only small thermal fluctuations around the average value in our supercell calculations. The coverage (θ) of the Al atoms in the transitional layer at different temperatures is listed in Table I. Here, full coverage (i.e., $\theta = 1$) corresponds to the perfect honeycombl-like lattice with no vacancies, and the average coverage was calculated to be about $\theta = 0.9$ at $T = 700$ – 1000 K. We also found that the density of the Al vacancies in the transitional layer does not depend much on the thickness of the Al nanofilm; for $t_{\text{Al}} = 1.76, 2.64$, and 3.39 nm, the average coverage

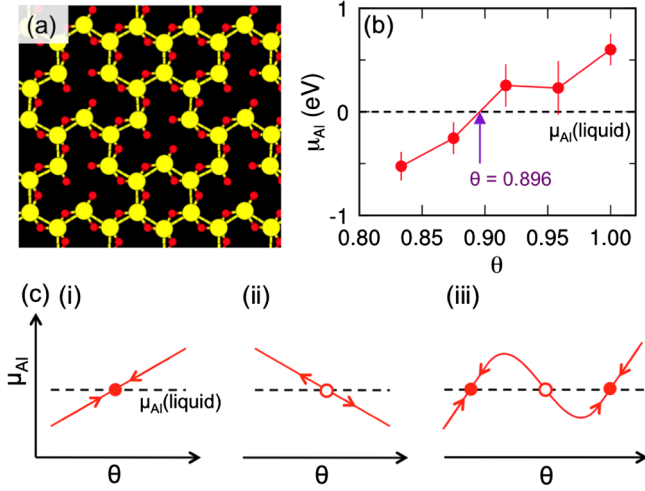


FIG. 2 (color online). Intrinsic vacancies in the honeycomb-like, transitional Al layer. (a) In-plane atomic ordering of the transitional Al layer at the interface. The O atoms in the O-terminated (0001) Al_2O_3 are also shown (Al: large balls, O: small balls). In (b), the Al chemical potential (μ_{Al}) is presented as a function of the Al coverage (θ) in the transitional layer with the liquid Al chemical potential, $\mu_{\text{Al}}(\text{liquid})$, set to zero. (c) Schematics of possible relations between the coverage θ and the chemical potential μ_{Al} that correspond to different interface morphologies (see text). Filled and open dots represent stable and unstable solutions, respectively.

at $T = 1000$ K was calculated to be $\theta = 0.906, 0.900$, and 0.903 , respectively.

At high temperature (e.g., $T = 1000$ K), the Al atoms frequently move back and forth between the transitional Al layer and the first liquid layer. Thus, in equilibrium, the chemical potential of Al atoms (μ_{Al}) in the transitional layer should be equal to that of the liquid Al phase, $\mu_{\text{Al}}(\text{liquid})$. Hence, the density of the Al vacancies at the transitional layer is determined by the equilibrium condition for Al atoms. To verify this, we calculated the μ_{Al} of the transitional layer as a function of the coverage θ [21], as shown in Fig. 2(b). Indeed, the equilibrium condition, $\mu_{\text{Al}}(\theta_{\text{eq}}) = \mu_{\text{Al}}(\text{liquid})$, gives the estimated coverage $\theta_{\text{eq}} = 0.896$, which is in excellent agreement with the result from the direct MD simulations, $\theta = 0.888\text{--}0.902$, in Table I.

TABLE I. Average atomic coverage (θ) in the transitional Al layer at different temperatures. Full coverage of $\theta = 1$ corresponds to the atomic arrangement of the perfect Al honeycomb lattice with no vacancies. The liquid states at $T = 700$ and 800 K correspond to supercooled liquid states below the melting point of the Al nanofilm ($T_m = 900$ K).

T (K)	700	800	900	1000
θ	0.888 ± 0.028	0.902 ± 0.028	0.895 ± 0.029	0.900 ± 0.029

Actually, the equilibrium condition, $\mu_{\text{Al}}(\theta_{\text{eq}}) = \mu_{\text{Al}}(\text{liquid})$, is only a necessary condition, but not a sufficient condition for the stable transitional Al layer. This is because the solution for the coverage θ_{eq} can be either stable or unstable depending on the sign of the slope $\gamma = d\mu_{\text{Al}}/d\theta$ at that coverage [Fig. 2(c)]; a positive slope γ leads to a negative-feedback regulation of the Al vacancies that opposes any change to the defect density, whereas a negative γ corresponds to a positive feedback effect that makes the corresponding equilibrium state unstable. This can be shown as follows. When θ deviates from θ_{eq} , the difference in the Al chemical potentials is given by $\Delta\mu = \mu_{\text{Al}}(\theta) - \mu_{\text{Al}}(\text{liquid}) = \gamma(\theta - \theta_{\text{eq}})$. If $\Delta\mu$ is positive, the Al atoms in the transitional Al layer move to the Al liquid phase to minimize the free energy of the system. As a result, the θ of the transitional layer decreases. If $\Delta\mu < 0$, the transitional layer accepts Al atoms from the liquid Al and the vacant sites are filled, leading to an increase in θ . Hence, if $\gamma > 0$, the deviation in θ becomes suppressed and θ is pinned to the equilibrium coverage [case (i) in Fig. 2(c)]. In contrast, for the system with negative γ as in

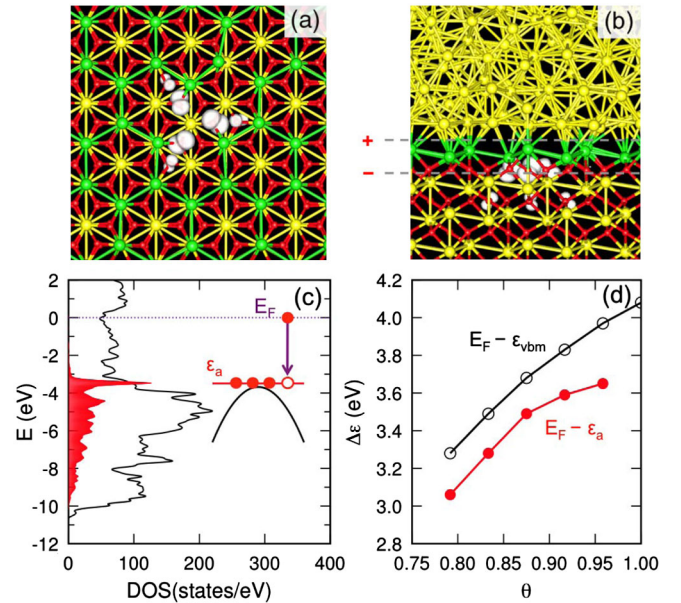


FIG. 3 (color online). Microscopic origin of the abrupt Al/ Al_2O_3 interface. The charge density plot of the defect levels of the Al vacancies (V_{Al}) at the interface: (a) top view and (b) side view. Large and small balls represent Al and O atoms, respectively. The Al atoms in the transitional layer are colored green. In (c), the total electronic density of states (DOS; solid line) of the Al/ Al_2O_3 interface is shown. The Fermi level (E_F) is set to zero. The shaded area represents the partial DOS projected on the O $2p$ orbitals near the V_{Al} , which is enlarged by a factor of 30 for better visibility. The schematic shown in the inset depicts the energy gain due to electron transfer from E_F to the V_{Al} acceptor level (ϵ_a) just above the Al_2O_3 VBM (ϵ_{VBM}) state. (d) The energy differences of the electronic levels, $E_F - \epsilon_a$ and $E_F - \epsilon_{\text{VBM}}$, are plotted as a function of the Al coverage (θ).

case (ii), a small deviation from θ_{eq} grows to either a high or low coverage state depending on the sign of the small deviation. Hence, there is no stable equilibrium state for the transitional Al layer, indicating that the atomically abrupt liquid-metal/oxide interface cannot be formed. If the interaction between the vacancies were sufficiently large, a system could have two stable solutions as in case (iii). Then, the transitional layer no longer would be a homogeneous phase, affecting the morphology of the solid-liquid interfaces.

Microscopic origin of the self-regulation of Al vacancies at the interface.—For the liquid Al/ Al_2O_3 interface, the slope γ is positive as shown in Fig. 2(b). Hence, a negative feedback is at work for the Al vacancies (V_{Al}) at the interface. To reveal the microscopic origin of the positive γ , we analyzed the electronic structures of the transitional interface layer with V_{Al} . As in bulk Al_2O_3 [22], the V_{Al} at the interface has defect levels above the valence band maximum (VBM) of Al_2O_3 . We found that due to reduced coordination the V_{Al} at the interface acts as a single acceptor, whereas the V_{Al} in the bulk Al_2O_3 is a triple acceptor. The localized defect states are characterized by the O $2p$ orbitals around the vacancy [Figs. 3(a) and 3(b)]. The V_{Al} at the interface is negatively charged because the defect level at ε_a accepts one electron from the Fermi level (E_F) of the liquid Al, as depicted in the inset of Fig. 3(c). This electron transfer lowers the formation energy of the V_{Al} by $\Delta\varepsilon = E_F - \varepsilon_a$, while breaking the Al-O and Al-Al bonds around the vacancy costs energy. The electron transfer from liquid Al also leads to the formation of an interfacial dipole layer [Fig. 3(b)]. The interfacial dipole moment in turn pushes the defect levels, as well as the valence bands of the Al_2O_3 , upwards with respect to E_F . Since the interfacial dipole strength is proportional to the density of the V_{Al} in the transitional layer, the energy gain due to the electron transfer, $\Delta\varepsilon = E_F - \varepsilon_a$, is reduced (enhanced) with increasing (decreasing) density of V_{Al} [Fig. 3(d)]. Therefore, upon any changes to the density of V_{Al} , the formation energy of V_{Al} is readjusted in a way that opposes the changes in the density; i.e., the chemical potential $\mu_{\text{Al}}(\theta)$ increases as the coverage θ increases (i.e., positive γ). Consequently, the coverage θ is pinned at a fixed value.

Liquid-phase epitaxial growth of Al_2O_3 .—The microscopic understanding of the liquid Al/(0001) α - Al_2O_3 (solid) interface suggests a possible mechanism of the layer-by-layer oxidation of the liquid Al, which was reported based on the *in situ* HRTEM measurements [9,11]. So far, we have assumed that there is no oxygen atom available in the liquid Al region. However, if oxygen atoms are provided externally through the space between the transitional Al layer and the first liquid layer, the oxygen atoms will form bonds with the Al atoms in the transitional layer. Because the binding energy of the newly formed Al-O bonds is larger than that of the metallic

Al-Al bonds, the chemical potential $\mu(\theta)$ decreases in the presence of the extra O atoms, reducing the interfacial energy [23]. We found that the positive μ_{Al} at $\theta = 1$ in Fig. 2(b) is lowered to -3.3 eV when the O coverage of the newly formed O (0001) layer is one. Therefore, as the oxidation proceeds, the coverage of the Al atoms in the transitional layer increases to $\theta = 1$. Simultaneously, on top of the newly formed O (0001) layer, a new transitional Al layer is formed with intrinsic Al vacancies ($\theta_{\text{eq}} = 0.9$), which completes the cycle of the layer-by-layer oxidation of the liquid Al.

In conclusion, our first-principles MD simulations reveal that the liquid Al/(0001) α - Al_2O_3 interface is atomically abrupt with a transitional Al layer. The transitional Al layer unexpectedly contains a large and almost fixed concentration of intrinsic Al vacancies (V_{Al}) of about 10 at. %. This puzzling observation can be explained by the electron transfer from the liquid Al to the transitional layer and the subsequent formation of an interfacial dipole layer with its dipole moment density proportional to the density of V_{Al} . The interfacial dipole field reduces the energy gain in the electron transfer, thus reducing the formation of V_{Al} . The self-regulation of the Al vacancies at the interface stabilizes the transitional Al layer and ultimately the atomically abrupt liquid-solid interface. This finding, therefore, should have far-reaching implications in understating the role of interfacial defects in the morphology of liquid-metal/metal-oxide interfaces and the associated growth processes.

This work was funded by the U.S. DOE EERE CSP Program and the NREL LDRD Program (Grant No. DE-AC36-08GO28308). This research used computing capabilities of the NREL CSC (Contract No. DE-AC36-08GO28308) and the NERSC (Contract No. DE-AC02-05CH11231). Y.-H.K. was supported by the WCU program (Grant No. R31-2008-000-10071-0) through the NRF of Korea.

*joongoo.kang@nrel.gov

- [1] S. J. Shin, J. Guzman, C.-W. Yuan, C. Y. Liao, C. N. Boswell-Koller, P. R. Stone, O. D. Dubon, A. M. Minor, M. Watanabe, J. W. Beeman, K. M. Yu, J. W. Ager III, D. C. Chrzan, and E. E. Haller, *Nano Lett.* **10**, 2794 (2010).
- [2] Y. Hong, S. Ding, W. Wu, J. Hu, A. A. Voevodin, L. Gschwendner, Ed. Snyder, L. Chow, and M. Su, *ACS Appl. Mater. Interfaces* **2**, 1685 (2010).
- [3] Q. Xu, I. D. Sharp, C. W. Yuan, D. O. Yi, C. Y. Liao, A. M. Glaeser, A. M. Minor, J. W. Beeman, M. C. Ridgway, P. Kluth, J. W. Ager III, D. C. Chrzan, and E. E. Haller, *Phys. Rev. Lett.* **97**, 155701 (2006).
- [4] C. Alba-Simionesco, B. Coasne, G. Dosseh, G. Dudziak, K. E. Gubbins, R. Radhakrishnan, and M. Sliwinski-Bartkowiak, *J. Phys. Condens. Matter Lett.* **18**, R15 (2006).

- [5] Q. S. Mei, S. C. Wang, H. T. Cong, Z. H. Jin, and K. Lu, *Phys. Rev. B* **70**, 125421 (2004).
- [6] X. W. Wang, G. T. Fei, K. Zheng, Z. Jin, and L. D. Zhang, *Appl. Phys. Lett.* **88**, 173114 (2006).
- [7] M. J. Regan, E. H. Kawamoto, S. Lee, P. S. Pershan, N. Maskil, M. Deutsch, O. M. Magnussen, B. M. Ocko, and L. E. Berman, *Phys. Rev. Lett.* **75**, 2498 (1995).
- [8] W. J. Huisman, J. F. Peters, M. J. Zwanenburg, S. A. de Vries, T. E. Derry, D. Abernathy, and J. F. van der Veen, *Nature (London)* **390**, 379 (1997).
- [9] S. H. Oh, Y. Kauffmann, C. Scheu, W. D. Kaplan, and M. Rühle, *Science* **310**, 661 (2005).
- [10] R. L. Davidchack and B. B. Laird, *Phys. Rev. Lett.* **85**, 4751 (2000).
- [11] S. H. Oh, M. F. Chisholm, Y. Kauffmann, W. D. Kaplan, W. Luo, M. Rühle, and C. Scheu, *Science* **330**, 489 (2010).
- [12] J. P. Perdew, K. Burke, and M. Ernzerhof, *Phys. Rev. Lett.* **77**, 3865 (1996).
- [13] G. Kresse and J. Furthmüller, *Phys. Rev. B* **54**, 11169 (1996).
- [14] P. E. Blöchl, *Phys. Rev. B* **50**, 17953 (1994).
- [15] G. Kresse and D. Joubert, *Phys. Rev. B* **59**, 1758 (1999).
- [16] S. Nosé, *J. Chem. Phys.* **81**, 511 (1984).
- [17] J. Kang and Y.-H. Kim, *ACS Nano* **4**, 1092 (2010).
- [18] J. Kang, S.-H. Wei, and Y.-H. Kim, *J. Am. Chem. Soc.* **132**, 18287 (2010).
- [19] Most of the calculations were done using NERSC HPC facilities with support of the U. S. DOE ASCR Leadership Computing Challenge (ALCC) program.
- [20] D. J. Siegel, L. G. Hector, Jr., and J. B. Adams, *Phys. Rev. B* **65**, 085415 (2002).
- [21] μ_{Al} was estimated by $\mu_{\text{Al}}(\theta) = E_{\text{tot}}(N) - E_{\text{tot}}(N-1) - \mu_{\text{Al}}(\text{liquid})$, where $E_{\text{tot}}(N)$ is the DFT total energy of the relaxed Al/Al₂O₃ supercells containing N atoms in the transitional Al layer, and $\theta = N/N_o$ for the number of Al atoms (N_o) in the perfect honeycomblake layer of the supercell. $E_{\text{tot}}(N)$ and $E_{\text{tot}}(N-1)$ are ensemble averaged over different MD structures and positions of Al vacancies.
- [22] K. Matsunaga, T. Tanaka, T. Yamamoto, and Y. Ikuhara, *Phys. Rev. B* **68**, 085110 (2003).
- [23] G. Levi and W. D. Kaplan, *Acta Mater.* **50**, 75 (2002).